

Multimodal brain-derived subtypes of Major depressive disorder differentiate patients for anergic symptoms, immune-inflammatory markers, history of childhood trauma and treatment-resistance

Federica Colombo^{1,2}, Federico Calesella², Beatrice Bravi^{1,2}, Lidia Fortaner-Uyà^{1,2}, Camilla Monopoli², Emma Tassi^{3,4}, Matteo Carminati¹, Raffaella Zanardi^{1,5}, Irene Bollettini², Sara Poletti^{1,2}, Cristina Lorenzi², Sara Spadini², Paolo Brambilla³, Alessandro Serretti⁶, Eleonora Maggioni⁴, Chiara Fabbri⁷, Francesco Benedetti^{1,2}, Benedetta Vai^{1,2}

1 University Vita-Salute San Raffaele, Milano, Italy

2 Psychiatry and Clinical Psychobiology Unit, Division of Neuroscience, IRCCS San Raffaele Hospital, Milano, Italy

3 Department of Neurosciences and Mental Health, IRCCS Fondazione Ca' Granda Ospedale Maggiore Policlinico, Milan, Italy

4 Politecnico di Milano, Department of Electronics, Information and Bioengineering, Milan, Italy

5 Mood Disorders Unit, Scientific Institute IRCCS San Raffaele Hospital, Milan, Italy

6 Department of Medicine and Surgery, Kore University of Enna, Enna, Italy

7 Department of Biomedical and Neuromotor Sciences, University of Bologna, Bologna, Italy.

To whom correspondence should be addressed:

Dr. Federica Colombo. M.Sc.

PhD student in Cognitive Neuroscience

Vita-Salute San Raffaele University

IRCCS Ospedale San Raffaele, Division of Neuroscience, Unit of psychiatry and clinical psychobiology

San Raffaele Turro, Via Stamira d'Ancona 20

Milano, Italy

Tel +39/02/26433156

Fax +39/02/26433265

E-mail: f.colombo8@studenti.univr.it

Abstract

An estimated 30% of Major Depressive Disorder (MDD) patients exhibit resistance to conventional antidepressant treatments. Identifying reliable biomarkers of treatment-resistant depression (TRD) represents a major goal of precision psychiatry, which is hampered by the clinical and biological heterogeneity. To uncover biologically-driven subtypes of MDD, we applied an unsupervised data-driven framework to stratify 102 MDD patients on their neuroimaging signature, including extracted measures of cortical thickness, grey matter volumes, and white matter fractional anisotropy. Our novel analytical pipeline integrated different machine learning algorithms to harmonize data, perform data dimensionality reduction, and provide a stability-based relative clustering validation. The obtained clusters were characterized for immune-inflammatory peripheral biomarkers, TRD, history of childhood trauma and depressive symptoms. Our results indicated two different clusters of patients, differentiable with 67% of accuracy: one cluster (n=59) was associated with a higher proportion of TRD, and higher scores of energy-related depressive symptoms, history of childhood abuse and emotional neglect; this cluster showed a widespread reduction in cortical thickness ($d=0.43-1.80$) and volumes ($d=0.45-1.05$), along with fractional anisotropy in the fronto-occipital fasciculus, stria terminalis, and corpus callosum ($d=0.46-0.52$); the second cluster (n=43) was associated with cognitive and affective depressive symptoms, thicker cortices and wider volumes. Multivariate analyses revealed distinct brain-inflammation relationships between the two clusters, with increase in pro-inflammatory markers being associated with decreased cortical thickness and volumes. Our stratification of MDD patients based on structural neuroimaging identified clinically-relevant subgroups of MDD with specific symptomatic and immune-inflammatory profiles, which can contribute to the development of tailored personalized interventions for MDD.

Accepted Author Manuscript
European Neuropsychopharmacology, 2024 Aug;
<https://doi.org/10.1016/j.euroneuro.2024.05.015>

Keywords: depression, machine learning, cluster analysis, neuroimaging, biomarkers

1. Introduction

Major depressive disorder (MDD) represents one of the most common psychiatric disorders worldwide, with almost 17% of men and 25% of women experiencing at least one lifetime depressive episode (Kessler et al., 2010). One of the most alarming issues contributing to the social and economic burden of the disorder is the uncertainty linked to clinical outcomes: despite the wide variability in treatment modalities, about 30% of patients do not achieve remission after antidepressant treatments (Conway et al., 2017) or relapse soon after, paving the way to treatment-resistant depression (TRD) (Sforzini et al., 2022). The lack of response to at least one antidepressant treatment is associated with more severe clinical outcomes, such as higher risk of suicide, more frequent relapses, psychiatric and medical comorbidities, health deterioration and functional impairment (Fekadu et al., 2009; Johnston et al., 2019). The prediction of clinical outcomes is further complicated by the absence of objective criteria for treatment choice, and several trials are often needed to find the optimal treatment for a patient (Rush et al., 2006). Indeed, a “precision psychiatry” approach to MDD is much-needed for the development of more effective treatments tailored on the individual profile.

One of the main obstacles hampering the development of personalized treatment strategies is the clinical and biological heterogeneity of MDD. At the symptoms level, the polythetic approach of current diagnostic systems uncovers multiple potential combinations of symptoms within MDD, with up to 227 possible ways to meet diagnostic criteria (Zimmerman et al., 2015). This variability in the clinical manifestation of MDD suggests the presence of several subtypes with unique etiologies and specific phenotypic profiles, despite their equivalence in terms of diagnostic label (Insel and Cuthbert, 2015). For instance, atypical depression is described by a unique symptomatology clearly distinguishable from melancholic and anxious depression (e.g., hypersomnia, increased appetite, and higher sensibility to rejection) (American Psychiatric Association, 2013), which is supposed to be driven by specific immunological and metabolic alterations occurring in this subtype (Lamers et al., 2018; Milaneschi et al., 2020). The understanding of the etiology of depression is further complicated by the multiple interactions among genetic, environmental, and lifestyle factors. In fact, although the heritability of MDD is estimated at 35-40% (Geschwind and Flint, 2015), approximately 67%

of variance in MDD is explained by environmental factors (Sullivan et al., 2000). An example of such factors is the experience of childhood trauma, which is considered as one of the strongest predictors of poor antidepressant response (Chekroud et al., 2016; Douglas and Porter, 2012; Williams et al., 2016). Compared to those not exposed to adverse childhood experiences, individuals with an history of childhood trauma typically have an earlier onset of MDD, more deleterious course, lower rates of remissions and response to treatments (Nanni et al., 2012; Teicher et al., 2022). At the biological level, adverse childhood experiences are supposed to induce a pro-inflammatory state that impact on neural circuits subserved to emotion regulation and processing (Baumeister et al., 2016; Gill et al., 2020; Nusslock and Miller, 2016; Rasmussen et al., 2020), promoting vulnerability for depression and unresponsiveness to antidepressant treatments (Fischer et al., 2021; Lippard and Nemeroff, 2020). In terms of neural correlates, structural neuroimaging studies indicate that volumetric changes in fronto-striatal and hippocampal volumes, together with reduced structural integrity in the corpus callosum and superior longitudinal fasciculus, differentiate TRD from treatment-responsive MDD and healthy controls (Klok et al., 2019; Runia et al., 2022). However, most of these findings failed to be consistently replicated, possibly due to the heterogeneity in the assessment of treatment resistance and in statistical methods (Miola and Meda, 2023).

As an attempt to uncover subgroups of psychiatric conditions, several studies employed unsupervised machine learning approaches in order to stratify patients based on shared characteristics (Dinga et al., 2018; Pelin et al., 2021; Wen et al., 2022). The most common approach is to apply unsupervised clustering algorithms on clinical data. While these studies suggest that specific symptoms-based clusters could be possibly linked to different effectiveness of antidepressant treatments (Chekroud et al., 2017; Kaster et al., 2023; Rost et al., 2023), the analysis of symptoms only is likely to be poorly informative given the very large heterogeneity of major depression clinical profile (Lorenzo-Luaces et al., 2021). An alternative approach is to identify biologically-driven subtypes by grouping patients based on shared neuro-biological features (Beijers et al., 2019). Recent studies applied clustering techniques on resting-state (Liang et al., 2020; Tokuda et al., 2018) and structural neuroimaging data (Yeung et al., 2021; Zhou et al., 2019), providing new

insights in how distinct neurobiological signatures could be linked to various clinical manifestations of depression. Despite the variability in the number of subtypes, most of the studies converge on the identification of anxiety-, anhedonia-, and insomnia-related data-driven clusters, as well as on clusters' differences in depression severity and recurrence (Buch and Liston, 2021). Some of these “biotypes” were found to be also predictive of response to antidepressant treatments (Drysdale et al., 2017), but these results were not replicated in independent samples (Dinga et al., 2019). Indeed, a common difficulty in the implementation of unsupervised algorithms is the lack of ground truth information and the absence of a defined approach to assess clustering validity, which further complicates the replicability of subtypes nested within clinical populations (Feczko et al., 2019). Moreover, none of these studies combined different neuroimaging modalities to investigate whether multimodal information could enhance the discovery of relevant subgroups.

In the current study, we aim to discover biologically-driven subtypes of patients based on multimodal structural neuroimaging, including grey matter volumes, cortical thickness, and extracted fractional anisotropy (FA) values of white matter tracts, in MDD patients. In order to overcome the methodological pitfalls highlighted in previous clustering studies (Dinga et al., 2019), we implemented a novel analytical pipeline including data harmonization, dimensionality reduction, and stability-based relative clustering validation to identify clusters of patients that are stable and generalizable to unseen observations (Landi et al., 2021). The rationale behind this approach is that if the discovered subtypes can be predicted in a new sample of patients, we would expect to find a similar stratification using the same type of data at the population level (Mandelli et al., 2023). The identified data-driven clusters were then profiled for immune inflammatory profiles and other clinical variables of interest, including TRD, depressive symptomatology, and history of childhood trauma.

2. Experimental procedures

2.1. Participants

A total of 102 recurrent and non-psychotic patients with a current diagnosis of MDD and an ongoing depressive episode were recruited at IRCCS San Raffaele Scientific Institute (Milan, Italy). In a subsample of 66 patients fasting blood samples were obtained between 7:00 to 9:00 for the quantification of peripheral immune analytes. Detailed inclusion and exclusion criteria are reported in Methods S1. After a complete description of the study, written informed consent was obtained. All procedures contributing to this work comply with the ethical standards of the relevant national and institutional committees on human experimentation and with the Helsinki Declaration of 1975, as revised in 2008. The study is approved by the local ethical committee.

2.2. Clinical and sociodemographic measures

Age, sex, number of previous mood episodes, age of onset (i.e., age when a first depressive episode occurred), duration of illness (i.e., number of years between the age of onset and the age at the recruitment), number of antidepressants and augmentation treatments, body mass index (BMI), and years of education were collected. To obtain a measure for pharmacological treatment, medication load for the last six months was calculated for each subject categorizing each medication into low-dose to high-dose groupings, scored as 0 (no medication), 1–4 (low to high dosages) as described by Sackeim (Sackeim, 2001) (see Methods S2 for detailed criteria). Lifetime treatment resistance was defined as a failure to respond to at least two antidepressant treatments of adequate dosages and duration (Brown et al., 2019; Sforzini et al., 2022; Thase and Rush, 1997). Despite several limitations of this definition has been highlighted (McAllister-Williams et al., 2020; Rush et al., 2019), these criteria are the most currently used in clinical practice for the identification of patients eligible for TRD interventions and it has been recently demonstrated to be particularly sensible in detecting the most severe MDD patients (Zanardi et al., 2024). Clinical data were assessed by the psychiatrist in charge using best estimation procedure, taking into account available charts, case notes, and information provided by at least one relative (Leckman et al., 1982). In a subsample of 64 patients, severity of depression was rated on the Beck Depression Inventory–Short Form (BDI-SF)

(Reynolds and Gould, 1981), and composite scores for different domains were derived: Negative Self-Esteem (items #3 (Sense of failure), #5 (Guilt), #7 (Self-hate), #8 (Suicide), and #10 (Body image)), Anergy (items #9 (Indecisiveness), #11 (Work inhibition), #12 (Fatigue), and #13 (Appetite)), and Dysphoria (items #1 (Sadness), #2 (Pessimism), #4 (Dissatisfaction), and #6 (Social withdrawal)) (Foelker Jr et al., 1987). Childhood trauma was evaluated using the 28-items Childhood Trauma Questionnaire (CTQ) (Bernstein et al., 2003). CTQ is a self-administrated inventory that was developed for a reliable retrospective assessment of neglect and abuse during childhood. The questionnaire is composed of 5 subscales that evaluate different aspects of neglect and abuse (physical, sexual, and emotional abuse, and physical and emotional neglect). Moreover, a Minimization/Denial validity scale was used to identify underreported maltreatment (Bernstein and Fink, 1998).

2.3. MRI data acquisition and pre-processing

All subjects underwent a magnetic resonance scan at C.E.R.M.A.C. (Centro di Eccellenza Risonanza Magnetica ad Alto Campo, University Vita-Salute San Raffaele, Milan, Italy). T1-weighted and diffusion tensor images (DTI) were acquired on two 3.0 Tesla scanners. Technical details for the two scanners are reported in Methods S3.

T1-weighted neuroanatomical images were processed using the Computational Anatomy Toolbox (CAT12) for SPM (Gaser and Dahnke, 2016). T1 images were normalized to an anatomical model and segmented into gray matter, white matter, and cerebrospinal fluid (CSF). Check of spatial alignment and sample homogeneity was performed to exclude outliers. Then, low-pass spatial filtering (smoothing) techniques were used to remove any potential artefacts in the tissue maps. Cortical thickness was derived for 68 regions defined by the Desikan-Killiany atlas (Desikan et al., 2006) and 148 from the Destrieux atlas (Destrieux et al., 2010), whereas volumes of cortical and subcortical grey matter volumes were extracted for 122 regions labelled by the Neuromorphometrics atlas (<http://Neuromorphometrics.com/>). Finally, total intracranial volume (TIV) was computed.

Whole-brain tract-wise average fractional anisotropy (FA) values were extracted according to ENIGMA-DTI protocols (<http://enigma.ini.usc.edu/protocols/dtiprotocols/>). DTI images were pre-processed using FMRIB Software Library (FSL) tools. Specifically, all volumes were corrected for eddy current induced distortions and subjects' movements (Horsfield, 1999). Then, a brain mask was created using Brain Extraction Tool (BET) (Smith, 2002), which deletes non-brain tissues from the image. Next, by FSL's DTIFIT command, included in FDT (Behrens et al., 2003), a voxel-wise diffusion tensor model was fit to the data in order to obtain parametric maps of FA. All subject's FA images were then processed using FSL's TBSS analytic method and were aligned to the MNI space, by using local deformation procedures performed by FMRIB's FNIRT. The mean of all aligned FA was then created, and a "thinning" process was applied to create a skeletonized mean FA image representing the centers of all common tracts. A threshold of 0.2 was set to this image in order to control for intersubject variability and reduce the likelihood of partial volume effect. Quality control, including inspections of data, vector gradients, registration, and average skeleton projection distance, were performed according to the ENIGMA-DTI protocol. Finally, all individual FA images were projected onto the skeleton by searching perpendicular from the skeleton for maximum FA values (Smith et al., 2006). Average FA values were calculated from voxels in each subject's white matter skeleton within 63 tract-wise ROIs, derived from the Johns Hopkins University (JHU) white matter parcellation atlas (Mori et al., 2008). FA values were separately calculated for right and left hemispheres in each ROI, except for body of corpus callosum (BCC), corpus callosum (CC), fornix (FX), genu of corpus callosum (GCC) and splenium of corpus callosum (SCC).

Since MRI data were acquired with two different scanners, we implemented the ComBat algorithm to correct for potential technical artefacts (i.e., "batch effects") that could affect meaningful relationships between biological signal and clinical outcomes, leading to unreliable conclusions (Fortin et al., 2017). The ComBat algorithm was adapted to be performed on regional gray matter estimates and extracted tract-based FA values. Of note, age, sex, and TIV (only for grey matter measures) were considered as biological covariates in order to be protected from the removal of scanner effects.

2.4. Laboratory determinants

In a subsample of 66 patients, Bio-Plex Pro™ Human Chemokine 40-Plex assays (BIO-RAD) was used for the identification of plasmatic concentrations of immune analytes, which were detected through the bead-based Luminex system according to xMAP technology (Luminex 200™ system, Merck Millipore). Analysed immune analytes included: a) cytokines: interleukin (IL)-1 β , IL-2, IL-4, IL-6, IL-10, IL-16, interferon (IFN)- γ , tumor necrosis factor (TNF)- α , macrophage migration inhibitory factor (MIF); b) chemokines: C-C motif ligand (CCL) 1, MCP-1/CCL2, MIP-1 α /CCL3, MCP-3/CCL7, MCP-2/CCL8, Eotaxin/CCL11, MCP-4/CCL13, MIP-1 δ /CCL15, TARC/CCL17, MIP-3 β /CCL19, MIP-3 α /CCL20, 6Ckine/CCL21, MDC/CCL22, MPIF-1/CCL23, Eotaxin-2/CCL24, Eotaxin-3/CCL26, TECK/CCL25, CTACK/CCL27, C-X-C motif chemokine ligand (CXCL) 1/ GRO- α , GRO- β /CXCL2, ENA-78/CXCL5, GCP-2/CXCL6, IL-8/CXCL8, CXCL9/MIG, IP-10/CXCL10, I-TAC/CXCL11, SDF-1 α + β /CXCL12, BCA-1/CXCL13, SCYB16/CXCL16, Fractalkine/CX3CL1; c) grow factors: granulocyte macrophage colony stimulating factor (GM-CSF). Median fluorescence intensities (MFI) of each analyte-specific immunoassay bead set were detected using the flow- and fluorescence-based Luminex 200™ detection platform (Luminex Corporation, Austin, TX, USA) (Vignali, 2000). We decided to use MFI instead of observed concentrations since there are no missing values and do not require a level of detection (LOD) (Breen et al., 2016). Moreover, MFI has been demonstrated to be more reliable than observed concentrations since some biases could be introduced in the interpolation of low signal values and has greater statistical power and greater discriminating compared to the observed concentration values (Breen et al., 2015; Breen et al., 2016). The intra-assay coefficients of variation (CV) was 4.3-26.2%, inter-assay CV was 54.7%. Given that samples were analyzed on different plates, we performed a normalization procedure on the log₂ transformed MFI values in order to control possible batch effects related to the plate.

2.5. Stability-based relative clustering validation

Clustering analyses were performed using the *reval* Python library

(https://github.com/IIT-LAND/reval_clustering), which implements a stability-based relative clustering approach within a cross-validation framework to identify the clustering solution that best replicates on unseen data (Landi et al., 2021). (For further details, see Methods S4). For the current study, *reval* was adapted to be used on neuroimaging features, choosing a Gaussian mixture model (GMM) with full covariance matrix as clustering algorithm, and support vector machine (SVM) as a supervised classifier. Given the high-dimensionality of the data, we performed the analyses both with and without dimensionality reduction to investigate the impact of multidimensionality on clustering performance (github repository: <https://github.com/fede-colombo/NeuReval>).

A graphic representation of the machine learning pipeline is depicted in Figure 1. In the first analysis, data were mean centered and normalized to the same scale. Input variables were adjusted for confounding effects of age, sex and TIV (only in grey matter) using linear regression. All these steps were fitted on the training set and then applied to the test set. A 2-folds cross-validation scheme (50% training, 50% test) was implemented to control for the size imbalance that derives from training-test splitting. The cross-validation scheme was repeated 10 times with 10 random labelling iterations to ensure robustness. To optimize the SVM hyperparameters (i.e., soft-margin C ranged 0.01, 0.1, 1, 10, 100, 1000) and the type of kernel (i.e., linear or radial), a grid search was performed in the training set and selection was based on normalized stability. Since previous studies identified from 2 to 4 clusters of MDD based on neuroimaging data (Buch and Liston, 2021), the entire cross-validation procedure was iterated over a number of GMM components from 2 to 5. The best clustering solution was the one that minimized the normalized stability throughout cross-validation. To assess the internal validity of the identified clusters, we also computed the silhouette and Davies-Bouldin scores by applying GMM on the entire dataset and with the same range of number of components used in the stability-based regime, and the adjusted mutual information (AMI) index was calculated to evaluate the similarity of clusters' labels derived from the stability-based approach and the ones obtained from silhouette and Davies-Bouldin scores model's selection.

Given the high-dimensionality of neuroimaging data, we repeated the same machine learning analyses by

applying Uniform Manifold Approximation and Projection (UMAP) for dimensionality reduction. UMAP is a novel nonlinear approach that employs manifold learning to map high dimensional data in a low dimensional space while preserving the global structure of the data (McInnes et al., 2018). Used as a preprocessing step, UMAP has been shown to boost the performance of different clustering algorithms, including GMM (Allaoui et al., 2020; Pandit et al., 2022; Yang et al., 2021). UMAP was initialized with a number of neighbors equal to 30, minimum distance equal to 0.0, and Euclidean distance metric, as suggested in the documentation (<https://umap-learn.readthedocs.io/en/latest/clustering.html>). Together with SVM hyperparameters, also the number of UMAP components was optimized within cross-validation through grid search in the training set, iterating over 2 to 5 components. As in the previous analysis, *reval* was run with 10 repetitions of 2-folds cross-validation and 10 random labelling (2-5 range of GMM components), and silhouette, Davies-Bouldin scores, and AMI index were calculated.

Despite the stability-based relative clustering approach allows us to assess the stability of a given clustering solution by means of cross-validation, it does not assess whether the identified clusters reflect the existence of true subgroups within the data. Therefore, we further investigated whether the selected clustering solutions significantly deviated from the null hypothesis that data derive from a single multivariate Gaussian distribution computed from 10,000 Monte Carlo simulations using the *sigclust* library in R (Huang et al., 2015).

2.6. Clinical, demographic, and neuroimaging characterization of the clusters

For both the analyses, the identified clusters were compared for neuroimaging features, TRD, age, sex, education, type of scanner, number of episodes, age of onset, duration of illness, medication load, BMI, CTQ total score and subscales, BDI total scores and domains, and HDRS-21 total score. Two-sample t-tests were performed for continuous variables, whereas χ^2 was calculated for categorical variables. For neuroimaging data, Cohen's d effects sizes were also computed and comparisons were deemed as significant if they passed a false-discovery rate (FDR) $q < 0.05$ threshold to correct for multiple comparisons.

To investigate whether the data-driven clusters reflect clinically-meaningful subgroups of depressed patients, we performed multivariate analysis of variance (MANOVA) considering BDI-SF domains, and CTQ subscales as dependent variables and clusters' labels as fixed factors. Age, sex, number of previous episodes, and medication load were entered as covariates to control for potential confounding effects. In case of significant results, subsequent linear discriminant analysis (LDA) was performed to assess how CTQ and BDI domains discriminate between the clusters. More specifically, the aim of LDA is to find a particular linear combination of dependent variables, also called as "variate", that best separate the identified clusters. Standardized coefficients were estimated to investigate the contribution of each CTQ and BDI domain to the discriminative variate. Finally, to investigate the interaction effect clusters-by-TRD on BDI and CTQ domains, we performed a non-parametric two-way MANOVA considering cluster's labels and TRD as fixed factors. All the analyses were performed in R using the *manova* (*jmv* library), *nparms* (*nparmD* library) and *lda* (*MASS* library) functions.

2.7. Multivariate brain-inflammation association analyses

To investigate univariate differences in immune-inflammatory markers between the identified clusters, non-parametric Mann-Whitney tests were performed assuming the non-normal distribution of the data. Multiple comparison correction was achieved with FDR $q < 0.05$. Together with univariate analyses, we also assess multivariate neuroimaging-inflammation within the discovered subtypes relationships through Partial Least Square Correlation (PLSC) analysis. PLSC has been widely applied in neuroimaging to investigate how variation in neuroimaging features covary with behavioral measures in a multivariate fashion (Kebets et al., 2019; Krishnan et al., 2011; Lombardo et al., 2021). The aim of PLSC is to identify latent variable (LV) pairs that maximize the covariance between brain and immune-inflammatory datasets that are also maximally uncorrelated with other brain-inflammation LV pairs. PLSC analyses were performed using the myPLS toolbox with MATLAB 2016b (<https://github.com/danizoeller/myPLS/>). For neuroimaging data, we considered grey mater volumes, cortical thickness, and extracted tract-based FA values, whereas all the 40

analytes were considered as immune-inflammatory markers. To compare brain-inflammation relationships between clusters, clusters' labels were entered as grouping structure in the PLS analyses. The confounding effect of age, sex, and TIV (only for grey matter measures) was regressed out from neuroimaging data before PLSC analyses separately for each cluster, whereas blood analytes concentrations were corrected for age, sex, and BMI. Statistical inference on LV pairs was achieved through permutation testing (5000 permutations). To limit the number of multiple comparisons, a FDR correction ($q < 0.05$) was applied on the first 5 LVs as previously suggested in literature (Kebets et al., 2019). Brain bootstrap ratios (BSR) and 95% confidence intervals (CI) on immune-inflammatory markers were estimated via bootstrap resampling (5000 resamples). BSR corresponds to the mean divided by the standard deviation of singular values (i.e., saliences) bootstrapped results, and they can be interpreted as Z-scores reflecting the impact of each brain variable on identified LVs. BRS higher than 2 were considered as relevant in driving brain-inflammation relationships, while immune-inflammatory loadings with 95%CI that do not include zero are considered as significant (Krishnan et al., 2011). Given the high-dimensionality of neuroimaging data, BRS were converted in p-values and a FDR correction ($q < 0.05$) was applied (Kebets et al., 2019). PLSC analyses were performed for both clustering solutions (with and without UMAP dimensionality reduction).

3. Results

3.1. Unsupervised data-driven identification of depression clusters based on neuroimaging data

The clinical and demographic characteristics of the sample are shown in Table 1. The stability-based relative validation clustering approach on multimodal structural neuroimaging data without data reduction identified that a 2-clusters solution minimized the normalized stability (0.316), showing a good discriminative performance with an accuracy of 68.4% (Figure 2B) (Table S1 in Supplementary Materials). The identified clustering solution deviated from the null hypothesis that clusters were generated from one single Gaussian distribution ($p = 0.035$). Density plot of the log probabilities estimated by the GMM model showed that, although the subtypes distributions are partially overlapping, they reflected two distinct Gaussian

distributions (Figure 2A). Similar results were obtained with UMAP dimensionality reduction (see Results S1 in Supplementary Materials).

3.2. Neurobiological-driven clusters are related to treatment response and specific neurobiological profiles

The identified clusters without UMAP data reduction were significantly different for TRD ($p=0.008$), sex ($p=0.03$), education ($p=0.016$), and number of augmentation treatments ($p=0.027$) (Table 2). Cluster 1 ($N=43$) was mainly composed by treatment-responsive patients whereas Cluster 2 ($N=59$) was characterized by higher TRD rates (Figure 2D). Notably, a higher F:M ratio was observed in Cluster 2 compared to Cluster 1. No significant differences in age, number of episodes, age of onset, duration of illness, and BMI was found between the two clusters (Table 2). Cortical thickness in temporo-parietal structures was significantly higher in Cluster 1 compared to Cluster 2 with a large effect size ($d=0.43-1.80$, $p_{FDR} < 0.001$) (Figure 3A). Considering gray matter volumes, the clusters were different with large effects in the bilateral thalami and parahippocampal gyrus, right middle occipital gyrus, right superior occipital gyrus, left temporal pole, right precuneus, right postcentral gyrus, left medial frontal cortex, left gyrus rectus, left precentral gyrus, and left superior parietal lobule, with higher volumes in Cluster 1 compared to Cluster 2 ($d=0.45-1.05$, $p_{FDR} < 0.001$) (Figure 3b). As for white matter, higher FA values were found in Cluster 1 compared to Cluster 2 (Figure 3C). Specifically, the right superior fronto-occipital fasciculus ($d=0.5$, $p_{FDR} = 0.032$), the body of the corpus callosum ($d=0.49$, $p_{FDR} = 0.024$), and the right stria terminalis ($d=0.46$, $p_{FDR} = 0.037$) differentiated the two clusters with a moderate effect (Table S2 in Supplementary Materials). A similar clustering solution was identified in the UMAP-reduced model (see Results S1 and Table S4 Supplementary Materials).

3.3. Neuroimaging-based subtypes reflect specific childhood trauma and depression-related signatures

The identified data-driven clusters reflected subtypes of depressed patients based on childhood trauma and depressive symptomatology using a multivariate approach. MANOVA results showed a significant between-

clusters difference (Wilks' $\lambda=0.68$, $F(9,50)=2.64$, $p=0.014$), considering age, sex, medication load, and number of episodes as nuisance covariates. Results from univariate statistics were not significant (Table 2). The following LDA identified one discriminant variate that significantly differentiated the two clusters (Wilks' $\lambda=0.70$, $p=0.013$). Standardized discriminant coefficients revealed that BDI Anergy ($b=1.48$), CTQ minimisation/denial ($b=1.23$), and CTQ emotional neglect ($b=1.07$) were largely positively associated with the variate, whereas Dysphoria ($b = -0.65$), Negative Self-Esteem ($b= -0.59$), and CTQ physical neglect ($b = -0.36$) showed a negative relationship with the variate (see Table S5 in Supplementary Materials for standardized coefficients for each BDI and CTQ domain). These results suggest that higher scores on the BDI Anergy, CTQ minimisation/denial and emotional neglect domains indicate a higher probability to be assigned to Cluster 2. Conversely, patients with higher scores on the BDI Dysphoria, Negative Self-Esteem, and CTQ physical neglect are more likely to belong to Cluster 1 (Figure 2C). No significant interaction effects between clusters' labels and TRD was found (Wilk's $\lambda=-2.81$, $p=0.998$). Similar findings were also obtained using clusters' labels derived from the UMAP-reduced model (see Results S1 and Table S6 in Supplementary Materials).

3.4. Differential multivariate brain-inflammation associations among clusters

We next investigated whether the discovered clusters are associated to different immune-inflammatory signatures (i.e., peripheral immune-inflammatory markers). None of these variables showed significant differences surviving to FDR correction between the two clusters (see Tables S7 and S8 in the Supplementary Materials). However, given the multivariate and high-dimensional nature of both imaging data and immune-inflammatory markers, PLSC analyses were performed to investigate whether the brain-inflammation relationships associated with each cluster might be better explained by a multivariate approach. A trend toward significance after FDR correction was observed for the first LV pair considering clusters' labels obtained from clustering analysis without UMAP dimensionality reduction ($p_{\text{FDR}}=0.058$). However, PLSC analyses entering clusters' labels derived from the UMAP-reduced model revealed a significant LV pairs surviving to FDR correction ($p_{\text{FDR}}=0.045$), which accounted for 27.39% brain-inflammation covariance.

Indeed, we focused on this last PLSC analysis for the rest of the manuscript. The contribution of neuroimaging variables on the identified LV was largely driven by a widespread effect of cortical thickness and grey matter volumes, with the largest BRS observed for thickness in the right lateral sulcus, right insula, and left pericalcarine cortex. Significant BRS were also observed for FA values in the internal and external capsule (Figure 4A-E). Considering the immune-inflammatory markers driving this relationship, there is evidence of a significant contribution of the majority of immune-inflammatory analytes in both clusters, especially in Cluster 2. Among them, CCL1, CCL26, and IL-6 showed the largest effects on the LV, with loadings higher than 0.9 in Cluster 2 (Figure 4F). These results suggest that, despite a strong brain-inflammation relationship can be found in both clusters, this association is stronger in a subtype of MDD patients characterized by anergic symptomatology and higher TRD rates. In both clusters, the direction of the loadings of the immune-inflammatory markers is negative, indicating that the increase in the concentrations of peripheral immune-inflammatory markers is associated with a decrease in cortical thickness and grey matter volumes.

4. Discussion

By implementing a novel cross-validated clustering procedure, we identified two subgroups of patients driven from grey matter and DTI features. Whereas one cluster was associated with energy-related depressive symptoms, history of childhood abuse and emotional neglect, and higher proportion of TRD, the other one was characterized by cognitive and affective depressive symptoms. The identified clusters were differentiable with an accuracy of 67%, suggesting that structural neuroimaging features can enhance the discovery of clinically-meaningful subtypes of depression.

Considering the clinical signatures of the identified subgroups, the BDI Anergy domain contributed the most in differentiating the two groups, reflecting a higher probability to belong to Cluster 2. Of note, this cluster includes more than 77% of TRD patients in our sample, suggesting an increased vulnerability to treatment resistant. Previous studies showed that symptoms reflecting an altered energy intake/output balance (e.g.,

appetite changes, sleep disturbances, and fatigue), characterize a specific MDD subtype characterized by altered immune-metabolic functions (Lamers et al., 2018; Milaneschi et al., 2020). In line with our stratification model, convergent evidence indicates that this symptomatology is more frequent in females with an early onset of diseases, recurrent episodes, and poor treatment outcomes (Vreijling et al., 2023). Also CTQ minimization/denial, emotional abuse and neglect scores contributed to discrimination between the two subtypes, reflecting a higher probability to belong to the “anergic” cluster. Previous evidence showed a possible link between childhood trauma and neurovegetative depressive symptomatology, reporting higher exposure to traumatic events in MDD patients with atypical features compared to those without (Withers et al., 2013). Indeed, it is possible that this cluster identifies a specific MDD subgroup with a higher sensitivity to early stress and more current anergic symptoms, in analogy to the extensive research documenting higher prevalence of anergic/atypical symptoms in reactive depression (Silverstein and Angst, 2015), both categories being less responsive to monoamine reuptake inhibitors (Quitkin et al., 1993; Stewart, 2007). Some these clinical features have been previously associated to a subthreshold vulnerability for bipolar disorder in MDD patients, which is also linked to an increased risk of TRD (Fornaro and Giosuè, 2010; Olgiati and Serretti, 2022). Future replication studies implementing a screening for subthreshold symptoms of bipolar disorder in MDD are needed to investigate the sensitivity of neuroimaging biomarkers in capturing the shared etiological mechanisms of Bipolar Disorder and TRD (Carta and Kalcev, 2023).

The hypothesis that the “anergic” cluster might be related to immune-metabolic dysfunctions is further supported by our results, which demonstrated differentially expressed inflammatory markers in the two clusters. Peripheral concentrations of immune-inflammatory markers were negatively associated with thickness and volumes in temporo-occipital structures, suggesting a detrimental effect of inflammation in the brain. This effect was evident in both clusters, which might reflect a continuum in the relationship between MDD neurobiology and inflammation in the brain-derived subtypes. However, the contribution of immune-inflammatory markers on the multivariate pattern was higher in the “anergic” cluster, with the largest effects observed for IL-1 β , CCL26, and CCL1. Although alterations in immune and adaptive immunity are

recognized within the MDD population (Beurel et al., 2020; Osimo et al., 2020), an increased production of pro-inflammatory markers seems to be peculiar to patients with atypical and non-melancholic symptoms (Lamers et al., 2018; Rothermundt et al., 2001) and more treatment-resistant (Chamberlain et al., 2019; Strawbridge et al., 2015). Polymorphisms and upregulated expression of IL-1 β genes have been consistently reported in MDD (Barnes et al., 2017; Heggul et al., 2013), representing a potential biomarker of less responsiveness to antidepressant treatments (Benedetti et al., 2021; Cattaneo et al., 2020; Cattaneo et al., 2016) especially for those with a history of childhood trauma (Ellul et al., 2016). The increase in peripheral IL-1 β levels has also been described in non-melancholic depression (Kaestner et al., 2005). Given the role of IL-1 β in stimulating cortisol release (Licinio and Frost, 2000) and evidence of hypothalamus-pituitary-adrenal (HPA) axis alterations in conditions reflecting atypical depressive symptoms (e.g., chronic fatigue syndrome) (Papadopoulos and Cleare, 2012), these findings are suggestive of a contribution of IL-1 β levels to the neurovegetative profile associated to the “anergic” cluster. Peripheral levels of CCL26 has been recently found to be increased in treatment-resistant MDD patients (Strawbridge et al., 2019), while its reduction after adjunctive minocycline treatment has been associated with poorer treatment outcome in BD (Soczynska et al., 2017). Despite being poorly explored in mood disorders, increased peripheral concentrations of CCL26 has been widely described in several neurodegenerative diseases (e.g., Alzheimer’s disease, amyotrophic lateral and multiple sclerosis, neuromyelitis optica, and Huntington’s disease), indicating a possible pro-inflammatory effect (e.g., damage of blood-brain barrier) contributing to degenerative processes in the brain (Du et al., 2021; Huber et al., 2018; Soares et al., 2012; Wild et al., 2011). Regarding CCL1, animal models studies suggest that mice deficient of the nod-like receptor protein 3 (NLRP-3) inflammasome, which promote depressive-like behaviours by triggering an inflammatory response in the brain (Alcocer-Gómez et al., 2014; Wong et al., 2016), exhibit decreased levels of IL-1 β and CCL1 in brain tissues, which correlates with a less susceptibility to depressive-like behaviours (Li et al., 2018b).

The data-driven subgroups also displayed distinct grey matter and structural connectivity profiles. Volumetric reductions in the precuneus, parahippocampal gyrus, thalamus, temporal pole, and pre- and

post-central gyri, were found in the “anergic” subtype. Most of these structures represent core areas in cortico-striatal-thalamic circuits, which are involved in attribution of salience to external stimuli, emotional regulation of inner states, and cognition (Bora et al., 2012; Price and Drevets, 2012). Aberrant inflammatory-mediated modulations in cortico-striatal pathways have been associated to increased negative affect and symptoms ascribable to atypical depression (e.g., hypersomnia, fatigue, social isolation, and psychomotor retardation), indicating a possible link between inflammation, metabolic alterations, dopamine neurotransmission, and depression (Felger et al., 2016; Goldsmith et al., 2020; Paul et al., 2023). When considering cortical thickness, the largest effects sizes were observed for temporo-parietal structures. Similar results were observed in a larger cohort study, where two MDD subgroups based on cortical thickness and surface reflected differences on general cognitive ability (Yeung et al., 2021). Our results take a step forward providing evidence of an association with other clinically meaningful measures. Together with grey matter, lower FA values in the superior fronto-occipital fasciculus, body of corpus callosum, stria terminalis, and hippocampal cingulum, were found in the “anergic” subtype. Microstructural changes in these tracts have been largely confirmed in depression literature, suggesting an inter-hemispheric and frontal-subcortical dysconnectivity in MDD (Chen et al., 2017; Van Velzen et al., 2020; Zhou et al., 2022). Among them, the stria terminalis is crucial in the regulation of the HPA activity, orchestrating the noradrenergic signaling among the amygdala, hippocampus, and the hypothalamus (Forray and Gysling, 2004). Given the discriminating value of anergic symptoms and childhood trauma between the identified clusters, it is possible that the different integrity of the stria terminalis might be related to the presence of neurovegetative symptoms in one cluster, reflecting a different involvement of the stria terminalis in modulating HPA response to stress.

Previous studies aimed at identifying subgroups of MDD patients using neuroimaging data, showing how the clinical heterogeneity of MDD can be disentangled based on shared neurobiological correlates (Beijers et al., 2019; Drysdale et al., 2017; Tokuda et al., 2018). By exploring the relationships with childhood trauma and treatment response, we demonstrated that the identified biologically-driven subtypes are informative

about relevant clinical features outside depressive symptomatology, providing a more comprehensive picture of the multifaceted manifestations of MDD. A large drawback of previous studies is the application of conventional clustering approaches tied to the specific data at hand, limiting the generalizability of the identified subtypes. Contrary, the clustering pipeline implemented in our study has the advantage to translate the unsupervised setting into a supervised classification problem, providing a measure of clusters' stability and replicability to unseen data through cross-validation. Our approach was able to identify two clusters of patients with a good accuracy (67%), indicating that structural neuroimaging data conveys information sufficient for a data-driven stratification that replicates in unseen observations. Furthermore, a high-value strength of this work is the clinical validation of the discovered clusters. Although the cross-sectional nature of this study limits to longitudinally evaluation of disease's progression of patients assigned to different clusters, our results suggest unique clinical profiles associated to each biologically-driven cluster, which could be useful for tailoring new effective treatments based on the patient's individual signature. For instance, patients assigned to the "anergic" cluster might benefit from antidepressant therapies inducing neuroplastic changes, such as electroconvulsive therapy (Bracht et al., 2023; Schmitgen et al., 2020), repetitive transcranial magnetic stimulation (Ge et al., 2022; Jannati et al., 2023), deep brain stimulation (Cattarinussi et al., 2022; Conner et al., 2022), and ketamine (Kopelman et al., 2023; Taraku et al., 2023), whereas treatments targeting the immune-metabolic pathways, such as physical exercise, diet or anti-inflammatory treatments, may be also useful in alleviating the energy-related symptoms (Hang et al., 2021; Rethorst et al., 2016). Furthermore, considering that this cluster was also associated with high scores for CTQ, this group may benefit from adjunctive psychotherapeutic interventions focused on trauma (Mannarino et al., 2014; Shapiro, 2001). On the other hand, psychotherapies targeting cognitive distortions, such as cognitive behavioral therapy, might represent optimal treatment options for patients assigned to the opposite cluster associated to a more cognitive depressive symptomatology (Li et al., 2018a; Wiles et al., 2013).

The limitations of the current study should be acknowledged. First, all patients were recruited in the same clinical center, limiting the possibility to extend our findings to other cohorts. However, the cross-validation

framework provides a good approximation of clusters' generalizability (Landi et al., 2021). Second, since all patients were under pharmacological treatment at the time of scanning, we cannot rule out long-lasting effects of drugs on neuroimaging features. Another limitation comes from the sample size, which further may limit results generalizability. Despite the cross-validation framework provides insights on the generalizability of the identified clusters, our stratification model should be evaluated in larger cohorts to overcome potential statistical power issues and provide realistic applications in clinical practice. Finally, we recognize that noise in biological data might have affected clustering solutions. It should be considered, though, that the pre-processing steps employed (e.g., ComBat harmonization) helped in mitigating this issue. In conclusion, our results indicate that structural neuroimaging data can be used to define novel subtypes of depression that are informative about treatment resistance, depressive symptomatology, and childhood trauma. A multimodal stratification including other kind of data (e.g., functional neuroimaging and genetic data) may improve the prediction of disease's outcomes, uncovering how different pathophysiological mechanisms interact with different clinical features of depression.

Role of the Funding Source

Funding for this study was provided by the Italian Ministry of Health (grant numbers GR 2019-12370616 and PNRR-MAD-2022-12375859). FB research is funded by Fondazione Cariplo RI0134 CARIPLO 2019. The funding agencies had no further role in study design; in the collection, analysis and interpretation of data; in the writing of the report; and in the decision to submit the paper for publication. The project related to this work is registered on ClinicalTrials.gov (ClinicalTrials.gov ID: NCT05816018).

Contributors

FCo and BV designed the study and wrote the protocol. FCo performed the machine learning analyses and wrote the first draft of the manuscript. FCo together with FCa, BB, ET and EM performed preprocessing of neuroimaging data. LFU, CM, MC, RZ, IB, SP, BV and FB were involved in subjects recruitment and collection of neuroimaging and clinical data. CL and SS performed Luminex quantification for peripheral immune analytes. CF, AS, PB, RZ, MC, BV and FB provided expert input in critically interpreting the results, contributing to manuscript drafting and revision. All authors contributed to and have approved the final manuscript.

Acknowledgement

None.

Competing Interests

CF was a speaker for Janssen. AS is or was a consultant/speaker for Abbott, Abbvie, Angelini, AstraZeneca, Clinical Data, Boehringer, Bristol-Myers Squibb, Eli Lilly, GlaxoSmithKline, Innovapharma, Italfarmaco, Janssen, Lundbeck, Naurex, Pfizer, Polifarma, Sanofi, Taliaz and Servier. All other authors declare that they have no conflicts of interest.

Captions

Figure 1. Schematic representation of the statistical analysis plan. A) *reval* algorithm pipeline. B) analysis pipeline for applying *reval* on neuroimaging data. Clusters' labels derived from the best clustering solution (i.e., minimum normalized stability) were used for MANOVA and clusters' comparisons on neuroimaging features and treatment response. Adapted from (Landi et al., 2021).

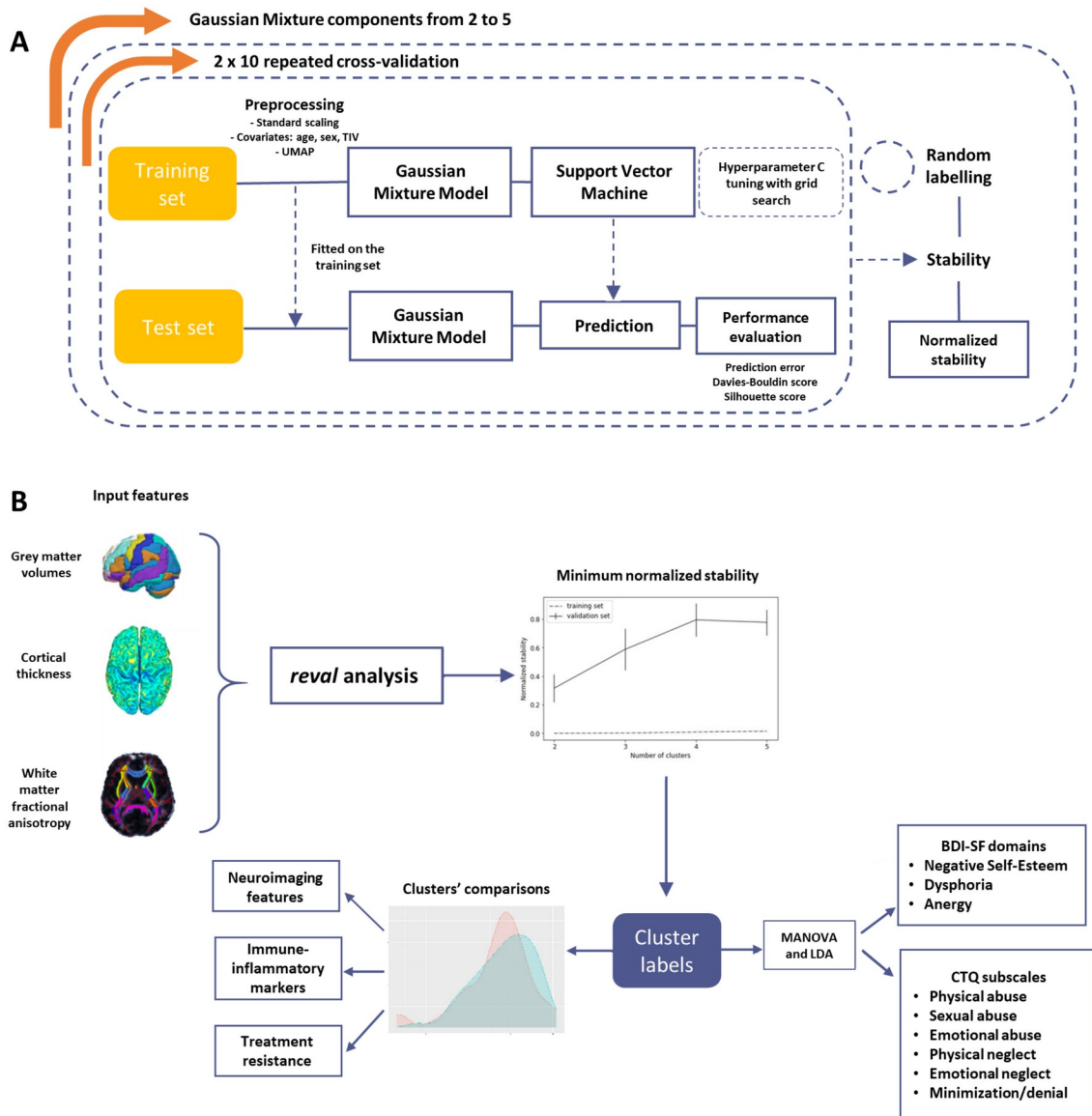


Figure 2. Unsupervised data-driven identification of depression subtypes based on neuroimaging data.

This figure represents results from the stability-based relative clustering approach. A) Probability density distributions identified by Gaussian Mixture Model and Support Vector Machine without UMAP data reduction. B) Normalized stability plot. Error bars represent the 95% confidence interval for normalized stability from the 10x2 repeated cross-validation. The optimal number of clusters that minimizes the normalized stability was 2, achieving an accuracy of 68%. C) Standardized coefficients of the linear discriminant analysis considering clusters' labels as fixed factors and BDI and CTQ domains as dependent variables. Positive weights (orange) reflect a higher probability to be assigned to Cluster 2, whereas negative weights (green) indicate a higher probability to belong to Cluster 1. D) Graphical representation of the proportion of TRD patients between the identified clusters.

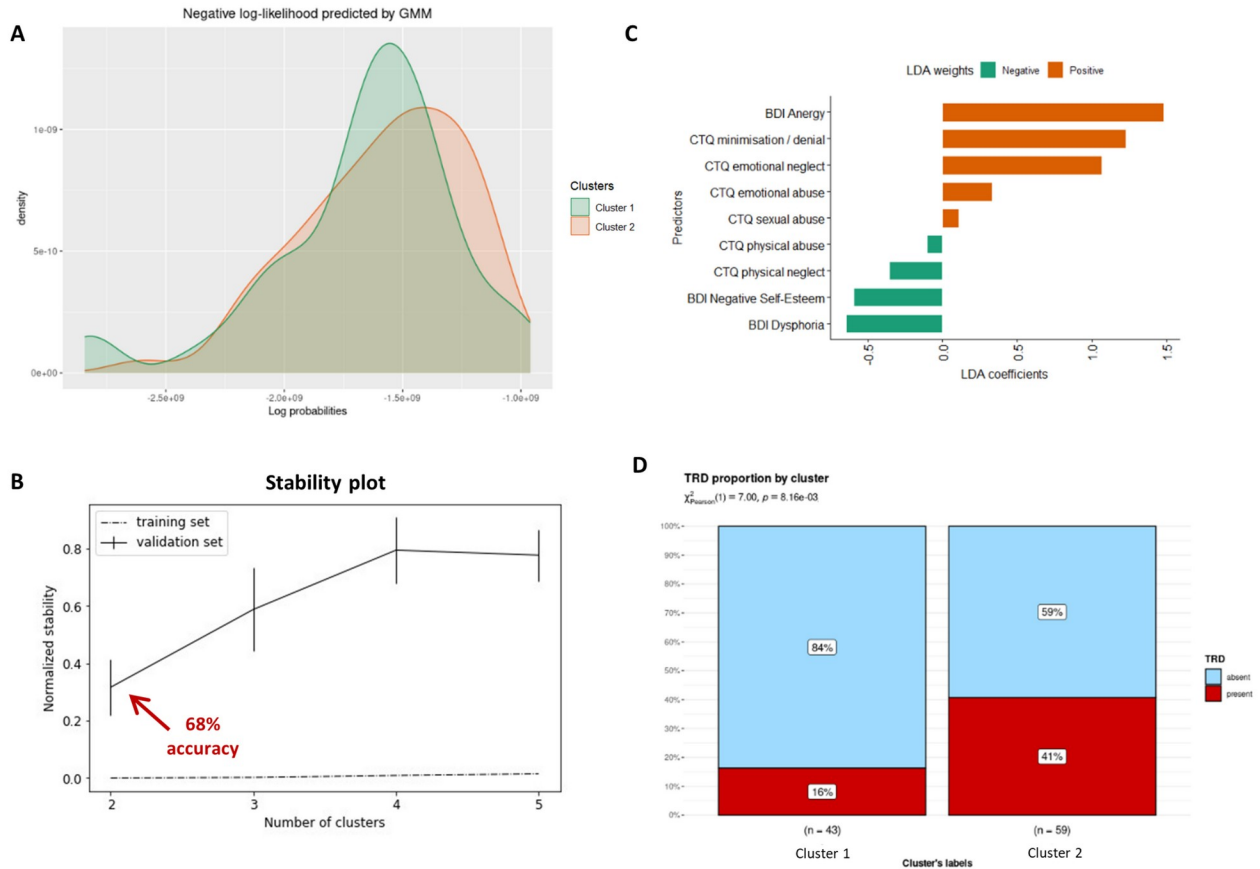


Figure 3. Standardized effect sizes differences (Cohen's d) in cortical, subcortical, and white matter structures associated with the identified clusters. Increasing red color indicates higher effect sizes (Cluster 1 > Cluster 2). A) Effect sizes for cortical thickness based on Destrieux (top) and Desikan-Killiany (down) atlases. B) Effect sizes for extracted tract-based FA values. C) Effect sizes for extracted grey matter volumes.

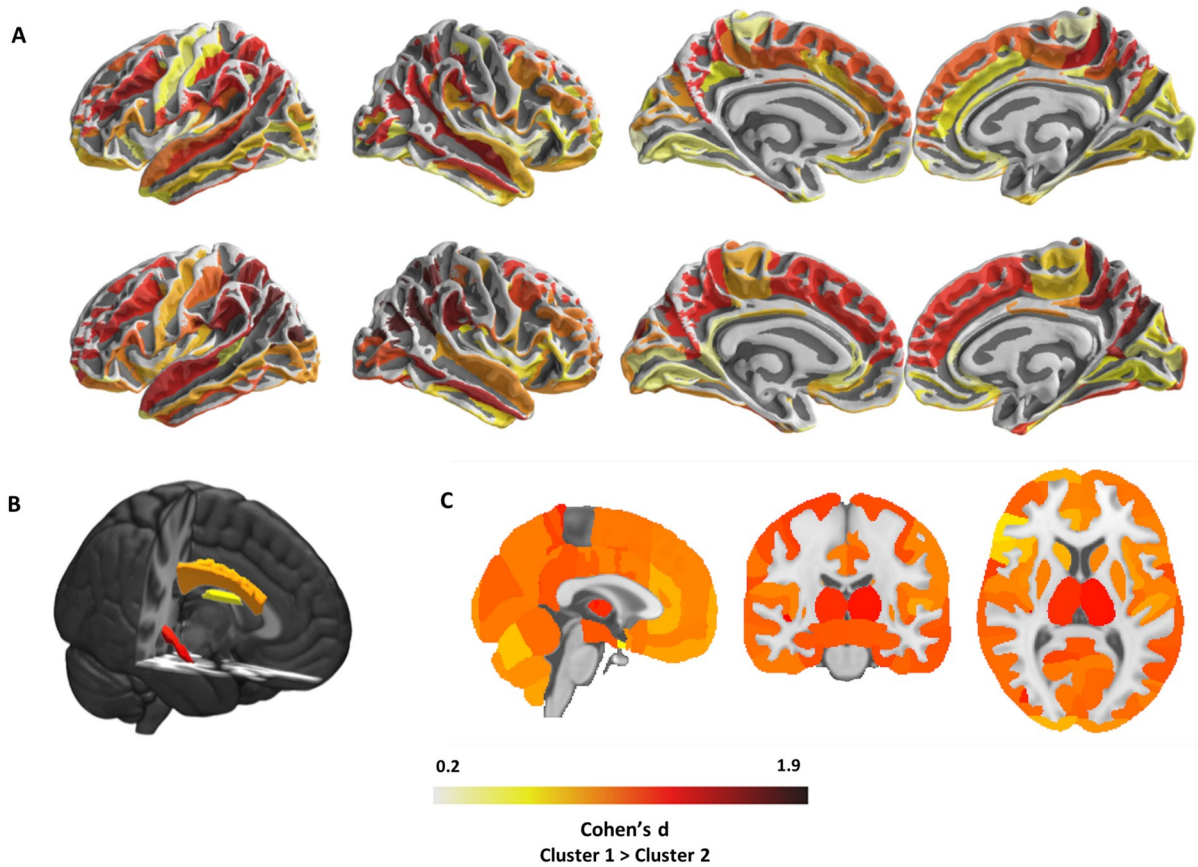
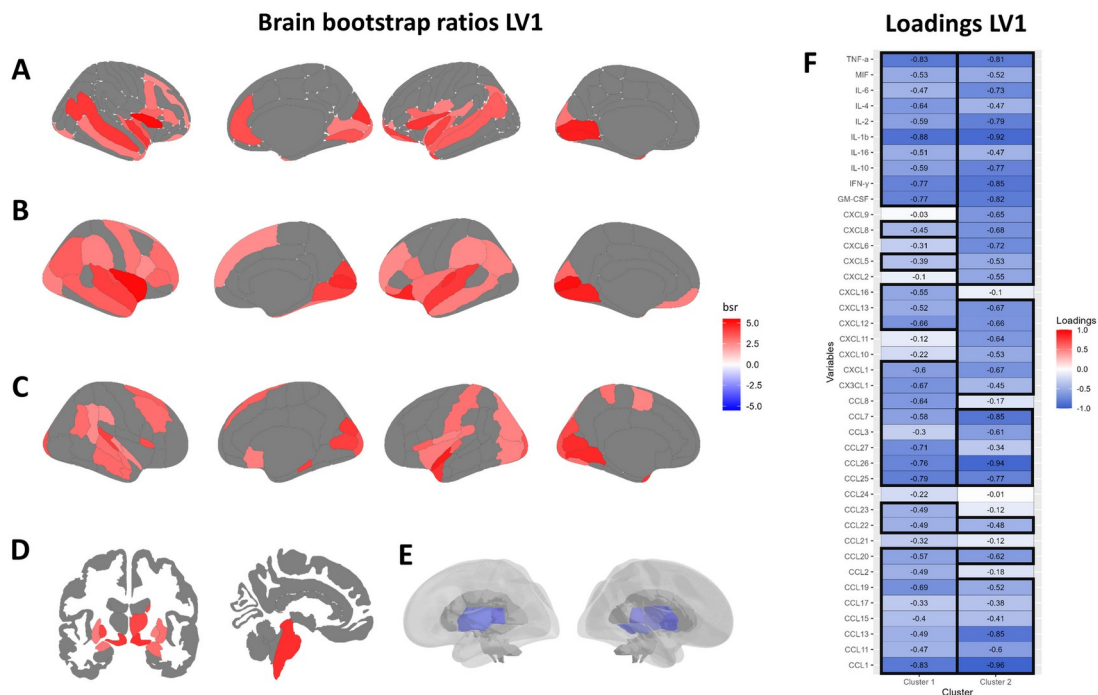


Figure 4. Differential brain-inflammation multivariate relationships between the identified clusters. PLSC analyses revealed one significant latent variable (LV1) that exhibit differential multivariate brain by

immune-inflammatory markers relationships between the two clusters. Panels from A to E show significant brain bootstrap ratios (BSRs) from LV1 for each neuroimaging modality (i.e., BSRs > 2), including cortical thickness based on Destrieux (A) and Desikan-Killiany atlas (B); grey matter cortical (C) and subcortical (D) volumes; extracted tract-based FA values (E). Panel F shows PLS loadings on the identified LV for each immune analyte (rows) and each cluster (columns). Stronger PLS loadings indicate immune analytes that are more important in driving the LV1 relationship. Cells with black outline indicate those correlations whose 95% confidence intervals do not include zero, representing reliable contributors to the LV1 relationships observed in the identified clusters.



Accepted Author Manuscript
European Neuropsychopharmacology, 2024 Aug;
<https://doi.org/10.1016/j.euroneuro.2024.05.015>

Table 1. Descriptive statistics of the whole sample

Participant Characteristics	mean (SD)
Age (years)	49.43 (10.00)
number of episodes	5.67 (6.21)
age of onset (years)	32.30 (11.78)
duration of illness (years)	17.13 (10.51)
Education (years)	12.75 (3.82)
medication load	4.57 (2.03)
Number of current antidepressant treatments	1.25 (0.62)
Number of current augmentation treatments^a	1.20 (1.04)
BMI	24.82 (5.27)
HDRS-21 total score	21.03 (5.91)
Participant Characteristics	Sample size
Sex	33 M, 69 F
Scanner acquisition^b	46 old, 56 new
TRD	71 non-TRD, 31 TRD

Abbreviations: SD, standard deviation; BMI, body mass index; TRD, treatment-resistant depression; HDRS, Hamilton Depression Rating Scale.

^a Augmentation treatments included low-dosage antipsychotics, light therapy, repeated transcranial magnetic stimulation (rTMS), hormonal and antiinflammatory treatments.

^b T1-weighted and diffusion tensor images were acquired on two 3.0 Tesla scanners. Until June 2016, 46 MDD patients were acquired with a Gyroscan Intera, Philips (old scanner). From October 2016, 56 MDD patients were examined with the Ingenia CX, Philips (new scanner).

Accepted Author Manuscript
European Neuropsychopharmacology, 2024 Aug;
<https://doi.org/10.1016/j.euroneuro.2024.05.015>

Table 2 Demographic and clinical characteristics of the identified data-driven clusters without UMAP dimensionality reduction.

Variable	Cluster 1 (N=43)	Cluster 2 (N=59)	t / χ^2	p
Age (years)	50.98 (8.73)	48.31 (10.77)	1.34	0.184
sex	19 M, 24 F	14 M, 45 F	4.76	0.03*
scanner	19 old, 24 new	27 old, 32 new	0.03	0.874
number of episodes	5.47 (5.15)	5.81 (6.91)	-0.28	0.781
age of onset (years)	33.93 (11.18)	31.12 (12.15)	1.19	0.236
duration of illness (years)	17.05 (11.05)	17.19 (10.19)	-0.07	0.947
Education (years)	11.70 (3.80)	13.53 (3.68)	-2.44	0.016*
medication load	4.35 (2.13)	4.71 (2.14)	-0.85	0.398
Number of current antidepressant treatments	1.37 (0.58)	1.15 (0.64)	1.78	0.078
Number of current augmentation treatments	0.93 (0.94)	1.39 (1.08)	-2.24	0.027*
BMI	25.29 (4.63)	24.99 (4.76)	0.32	0.375
TRD	36 non-TRD, 7 TRD	35 non-TRD, 24 TRD	7.00	0.008**
HDRS-21 total score	23.19 (7.26)	22.27 (7.00)	0.64	0.522
CTQ total score ^a	44.92 (15.04)	41.40 (13.41)	0.94	0.351
CTQ physical abuse ^a	6.25 (2.47)	6.13 (2.46)	0.20	0.845
CTQ emotional neglect ^a	13.83 (5.54)	12.90 (5.27)	0.67	0.504
CTQ emotional abuse ^a	9.38 (4.54)	8.93 (4.31)	0.40	0.693
CTQ physical neglect ^a	8.54 (4.03)	7.03 (3.04)	1.71	0.093
CTQ sexual abuse ^a	6.08 (3.51)	6.18 (3.38)	-0.10	0.918
CTQ minimization/denial ^a	7.92 (3.13)	9.40 (3.05)	-1.86	0.067
BDI total score ^a	16.13 (8.96)	16.73 (7.74)	-0.28	0.778

BDI Self-Esteem^a	5.92 (3.48)	5.80 (3.08)	0.14	0.889
BDI Anergy^a	4.79 (3.02)	6.15 (2.53)	-1.93	0.058
BDI Dysphoria^a	5.42 (3.62)	5.20 (2.70)	0.27	0.784

Results for continuous variables are reported as mean (standard deviation), whereas sample size is reported for categorical variables. Abbreviations: BMI, body mass index; TRD, treatment-resistant depression; HDRS-21, 21-Hamilton Depression Rating Scale; CTQ, Childhood Trauma Questionnaire; BDI, Beck Depression Inventory.

^a subsample of 64 MDD patients with clinical scales (cluster 1: N=24; cluster 2: N=40). *p<0.05, **p<0.001

References

- Alcocer-Gómez, E., de Miguel, M., Casas-Barquero, N., Núñez-Vasco, J., Sánchez-Alcazar, J.A., Fernández-Rodríguez, A., Cordero, M.D., 2014. NLRP3 inflammasome is activated in mononuclear blood cells from patients with major depressive disorder. *Brain. Behav. Immun.* 36, 111-117.
- Allaoui, M., Kherfi, M.L., Cheriet, A., 2020. Considerably improving clustering algorithms using UMAP dimensionality reduction technique: a comparative study, *Image and Signal Processing: 9th International Conference, ICISP 2020, Marrakesh, Morocco, June 4–6, 2020, Proceedings 9*. Springer, pp. 317-325.
- American Psychiatric Association, 2013. *Diagnostic and statistical manual of mental disorders: DSM-5™*, 5th ed. American Psychiatric Publishing, Inc., Arlington, VA, US.
- Barnes, J., Mondelli, V., Pariante, C.M., 2017. Genetic Contributions of Inflammation to Depression. *Neuropsychopharmacology* 42, 81-98.
- Baumeister, D., Akhtar, R., Ciufolini, S., Pariante, C.M., Mondelli, V., 2016. Childhood trauma and adulthood inflammation: a meta-analysis of peripheral C-reactive protein, interleukin-6 and tumour necrosis factor- α . *Mol. Psychiatry* 21, 642-649.
- Behrens, T.E., Woolrich, M.W., Jenkinson, M., Johansen-Berg, H., Nunes, R.G., Clare, S., Matthews, P.M., Brady, J.M., Smith, S.M., 2003. Characterization and propagation of uncertainty in diffusion-weighted MR imaging. *Magnetic Resonance in Medicine: An Official Journal of the International Society for Magnetic Resonance in Medicine* 50, 1077-1088.
- Beijers, L., Wardenaar, K.J., van Loo, H.M., Schoevers, R.A., 2019. Data-driven biological subtypes of depression:

- systematic review of biological approaches to depression subtyping. *Molecular psychiatry* 24, 888-900.
- Benedetti, F., Poletti, S., Vai, B., Mazza, M.G., Lorenzi, C., Brioschi, S., Aggio, V., Branchi, I., Colombo, C., Furlan, R., 2021. Higher baseline interleukin-1 β and TNF- α hamper antidepressant response in major depressive disorder. *Eur. Neuropsychopharmacol.* 42, 35-44.
- Bernstein, D.P., Stein, J.A., Newcomb, M.D., Walker, E., Pogge, D., Ahluvalia, T., Stokes, J., Handelsman, L., Medrano, M., Desmond, D., 2003. Development and validation of a brief screening version of the Childhood Trauma Questionnaire. *Child Abuse Negl.* 27, 169-190.
- Bernstein, D.P., Fink, L., 1998. *Childhood trauma questionnaire: A retrospective self-report.* The Psychological Corporation: San Antonio.
- Beurel, E., Toups, M., Nemeroff, C.B., 2020. The bidirectional relationship of depression and inflammation: double trouble. *Neuron* 107, 234-256.
- Bora, E., Harrison, B.J., Davey, C.G., Yücel, M., Pantelis, C., 2012. Meta-analysis of volumetric abnormalities in cortico-striatal-pallidal-thalamic circuits in major depressive disorder. *Psychol. Med.* 42, 671-681.
- Bracht, T., Walther, S., Breit, S., Mertse, N., Federspiel, A., Meyer, A., Soravia, L.M., Wiest, R., Denier, N., 2023. Distinct and shared patterns of brain plasticity during electroconvulsive therapy and treatment as usual in depression: an observational multimodal MRI-study. *Transl. Psychiatry* 13, 6.
- Breen, E.J., Polaskova, V., Khan, A., 2015. Bead-based multiplex immuno-assays for cytokines, chemokines, growth factors and other analytes: median fluorescence intensities versus their derived absolute concentration values for statistical analysis. *Cytokine* 71, 188-198.
- Breen, E.J., Tan, W., Khan, A., 2016. The statistical value of raw fluorescence signal in Luminex xMAP based multiplex immunoassays. *Sci. Rep.* 6, 26996.
- Brown, S., Rittenbach, K., Cheung, S., McKean, G., MacMaster, F.P., Clement, F., 2019. Current and Common Definitions of Treatment-Resistant Depression: Findings from a Systematic Review and Qualitative Interviews. *The Canadian Journal of Psychiatry* 64, 380-387.
- Buch, A.M., Liston, C., 2021. Dissecting diagnostic heterogeneity in depression by integrating neuroimaging and genetics. *Neuropsychopharmacology* 46, 156-175.
- Carta, M.G., Kalcev, G., 2023. Screening, Genetic Variants, and Bipolar Disorders: Can Useful Hypotheses Arise from the Sum of Partial Failures? *13*, 853-862.

Cattaneo, A., Ferrari, C., Turner, L., Mariani, N., Enache, D., Hastings, C., Kose, M., Lombardo, G., McLaughlin, A.P., Nettis, M.A., Nikkheslat, N., Sforzini, L., Worrell, C., Zajkowska, Z., Cattane, N., Lopizzo, N., Mazzelli, M., Pointon, L., Cowen, P.J., Cavanagh, J., Harrison, N.A., de Boer, P., Jones, D., Drevets, W.C., Mondelli, V., Bullmore, E.T., Pariante, C.M., the Neuroimmunology of Mood, D., Alzheimer's Disease, C., 2020. Whole-blood expression of inflammasome- and glucocorticoid-related mRNAs correctly separates treatment-resistant depressed patients from drug-free and responsive patients in the BIODIEP study. *Transl. Psychiatry* 10, 232.

Cattaneo, A., Ferrari, C., Uher, R., Bocchio-Chiavetto, L., Riva, M.A., Consortium, t.M.I., Pariante, C.M., 2016. Absolute Measurements of Macrophage Migration Inhibitory Factor and Interleukin-1- β mRNA Levels Accurately Predict Treatment Response in Depressed Patients. *Int. J. Neuropsychopharmacol.* 19.

Cattarinussi, G., Moghaddam, H.S., Aarabi, M.H., Squarcina, L., Sambataro, F., Brambilla, P., Delvecchio, G., 2022. White Matter Microstructure Associated with the Antidepressant Effects of Deep Brain Stimulation in Treatment-Resistant Depression: A Review of Diffusion Tensor Imaging Studies. *International Journal of Molecular Sciences* 23, 15379.

Chamberlain, S.R., Cavanagh, J., De Boer, P., Mondelli, V., Jones, D.N., Drevets, W.C., Cowen, P.J., Harrison, N.A., Pointon, L., Pariante, C.M., 2019. Treatment-resistant depression and peripheral C-reactive protein. *BJPsych* 214, 11-19.

Chekroud, A.M., Gueorguieva, R., Krumholz, H.M., Trivedi, M.H., Krystal, J.H., McCarthy, G., 2017. Reevaluating the efficacy and predictability of antidepressant treatments: a symptom clustering approach. *JAMA psychiatry* 74, 370-378.

Chekroud, A.M., Zotti, R.J., Shehzad, Z., Gueorguieva, R., Johnson, M.K., Trivedi, M.H., Cannon, T.D., Krystal, J.H., Corlett, P.R., 2016. Cross-trial prediction of treatment outcome in depression: a machine learning approach. *Lancet Psychiatry* 3, 243-250.

Chen, G., Guo, Y., Zhu, H., Kuang, W., Bi, F., Ai, H., Gu, Z., Huang, X., Lui, S., Gong, Q., 2017. Intrinsic disruption of white matter microarchitecture in first-episode, drug-naive major depressive disorder: A voxel-based meta-analysis of diffusion tensor imaging. *Prog. Neuropsychopharmacol. Biol. Psychiatry* 76, 179-187.

Conner, C.R., Quevedo, J., Soares, J.C., Fenoy, A.J., 2022. Brain metabolic changes and clinical response to superolateral medial forebrain bundle deep brain stimulation for treatment-resistant depression. *Mol. Psychiatry*, 1-7.

Conway, C.R., George, M.S., Sackeim, H.A., 2017. Toward an evidence-based, operational definition of treatment-

resistant depression: when enough is enough. *JAMA psychiatry* 74, 9-10.

Desikan, R.S., Ségonne, F., Fischl, B., Quinn, B.T., Dickerson, B.C., Blacker, D., Buckner, R.L., Dale, A.M., Maguire, R.P., Hyman, B.T., 2006. An automated labeling system for subdividing the human cerebral cortex on MRI scans into gyral based regions of interest. *Neuroimage* 31, 968-980.

Destrieux, C., Fischl, B., Dale, A., Halgren, E., 2010. Automatic parcellation of human cortical gyri and sulci using standard anatomical nomenclature. *Neuroimage* 53, 1-15.

Dinga, R., Marquand, A.F., Veltman, D.J., Beekman, A.T., Schoevers, R.A., van Hemert, A.M., Penninx, B.W., Schmaal, L., 2018. Predicting the naturalistic course of depression from a wide range of clinical, psychological, and biological data: a machine learning approach. *Transl. Psychiatry* 8, 241.

Dinga, R., Schmaal, L., Penninx, B.W., van Tol, M.J., Veltman, D.J., van Velzen, L., Mennes, M., van der Wee, N.J., Marquand, A.F., 2019. Evaluating the evidence for biotypes of depression: Methodological replication and extension of. *NeuroImage: Clinical* 22, 101796.

Douglas, K.M., Porter, R.J., 2012. The effect of childhood trauma on pharmacological treatment response in depressed inpatients. *Psychiatry Res.* 200, 1058-1061.

Drysdale, A.T., Grosenick, L., Downar, J., Dunlop, K., Mansouri, F., Meng, Y., Fetcho, R.N., Zebley, B., Oathes, D.J., Etkin, A., 2017. Resting-state connectivity biomarkers define neurophysiological subtypes of depression. *Nat. Med.* 23, 28-38.

Du, L., Chang, H., Xu, W., Zhang, X., Yin, L., 2021. Elevated chemokines and cytokines for eosinophils in neuromyelitis optica spectrum disorders. *Multiple Sclerosis and Related Disorders* 52, 102940.

Ellul, P., Boyer, L., Groc, L., Leboyer, M., Fond, G., 2016. Interleukin-1 β -targeted treatment strategies in inflammatory depression: toward personalized care. *Acta Psychiatr. Scand.* 134, 469-484.

Feczko, E., Miranda-Dominguez, O., Marr, M., Graham, A.M., Nigg, J.T., Fair, D.A., 2019. The heterogeneity problem: Approaches to identify psychiatric subtypes. *TiCS* 23, 584-601.

Fekadu, A., Wooderson, S.C., Markopoulo, K., Donaldson, C., Papadopoulos, A., Cleare, A.J., 2009. What happens to patients with treatment-resistant depression? A systematic review of medium to long term outcome studies. *J. Affect. Disord.* 116, 4-11.

Felger, J.C., Li, Z., Haroon, E., Woolwine, B.J., Jung, M.Y., Hu, X., Miller, A.H., 2016. Inflammation is associated with decreased functional connectivity within corticostriatal reward circuitry in depression. *Mol. Psychiatry* 21, 1358-

1365.

Fischer, K.F., Simon, M.S., Elsner, J., Dobmeier, J., Dorr, J., Blei, L., Zill, P., Obermeier, M., Musil, R., 2021. Assessing the links between childhood trauma, C-reactive protein and response to antidepressant treatment in patients with affective disorders. *Eur. Arch. Psychiatry Clin. Neurosci.* 271, 1331-1341.

Foelker Jr, G.A., Shewchuk, R.M., Niederehe, G., 1987. Confirmatory factor analysis of the short form Beck Depression Inventory in elderly community samples. *J. Clin. Psychol.* 43, 111-118.

Fornaro, M., Giosuè, P., 2010. Current nosology of treatment resistant depression: a controversy resistant to revision. *Clin. Pract. Epidemiol. Ment. Health* 6, 20-24.

Fornay, M.I., Gysling, K., 2004. Role of noradrenergic projections to the bed nucleus of the stria terminalis in the regulation of the hypothalamic–pituitary–adrenal axis. *Brain Research Reviews* 47, 145-160.

Fortin, J.-P., Parker, D., Tunç, B., Watanabe, T., Elliott, M.A., Ruparel, K., Roalf, D.R., Satterthwaite, T.D., Gur, R.C., Gur, R.E., Schultz, R.T., Verma, R., Shinohara, R.T., 2017. Harmonization of multi-site diffusion tensor imaging data. *Neuroimage* 161, 149-170.

Gaser, C., Dahnke, R., 2016. CAT-a computational anatomy toolbox for the analysis of structural MRI data. *Hbm 2016*, 336-348.

Ge, R., Humaira, A., Gregory, E., Alamian, G., MacMillan, E.L., Barlow, L., Todd, R., Nestor, S., Frangou, S., Vila-Rodriguez, F., 2022. Predictive value of acute neuroplastic response to rTMS in treatment outcome in depression: a concurrent TMS-fMRI trial. *American Journal of Psychiatry* 179, 500-508.

Geschwind, D.H., Flint, J., 2015. Genetics and genomics of psychiatric disease. *Science* 349, 1489-1494.

Gill, H., El-Halabi, S., Majeed, A., Gill, B., Lui, L.M.W., Mansur, R.B., Lipsitz, O., Rodrigues, N.B., Phan, L., Chen-Li, D., McIntyre, R.S., Rosenblat, J.D., 2020. The Association Between Adverse Childhood Experiences and Inflammation in Patients with Major Depressive Disorder: A Systematic Review. *J. Affect. Disord.* 272, 1-7.

Goldsmith, D.R., Bekhbat, M., Le, N.-A., Chen, X., Woolwine, B.J., Li, Z., Haroon, E., Felger, J.C., 2020. Protein and gene markers of metabolic dysfunction and inflammation together associate with functional connectivity in reward and motor circuits in depression. *Brain. Behav. Immun.* 88, 193-202.

Hang, X., Zhang, Y., Li, J., Li, Z., Zhang, Y., Ye, X., Tang, Q., Sun, W., 2021. Comparative efficacy and acceptability of anti-inflammatory agents on major depressive disorder: a network meta-analysis. *Frontiers in Pharmacology* 12, 691200.

- Hepgul, N., Cattaneo, A., Zunszain, P.A., Pariante, C.M., 2013. Depression pathogenesis and treatment: what can we learn from blood mRNA expression? *BMC Med.* 11, 28.
- Horsfield, M.A., 1999. Mapping eddy current induced fields for the correction of diffusion-weighted echo planar images. *Magn. Reson. Imaging* 17, 1335-1345.
- Huang, H., Liu, Y., Yuan, M., Marron, J., 2015. Statistical significance of clustering using soft thresholding. *Journal of Computational and Graphical Statistics* 24, 975-993.
- Huber, A.K., Giles, D.A., Segal, B.M., Irani, D.N., 2018. An emerging role for eotaxins in neurodegenerative disease. *Clin. Immunol.* 189, 29-33.
- Insel, T.R., Cuthbert, B.N., 2015. Brain disorders? precisely. *Science* 348, 499-500.
- Jannati, A., Oberman, L.M., Rotenberg, A., Pascual-Leone, A., 2023. Assessing the mechanisms of brain plasticity by transcranial magnetic stimulation. *Neuropsychopharmacology* 48, 191-208.
- Johnston, K.M., Powell, L.C., Anderson, I.M., Szabo, S., Cline, S., 2019. The burden of treatment-resistant depression: a systematic review of the economic and quality of life literature. *J. Affect. Disord.* 242, 195-210.
- Kaestner, F., Hettich, M., Peters, M., Sibrowski, W., Hetzel, G., Ponath, G., Arolt, V., Cassens, U., Rothermundt, M., 2005. Different activation patterns of proinflammatory cytokines in melancholic and non-melancholic major depression are associated with HPA axis activity. *J. Affect. Disord.* 87, 305-311.
- Kaster, T.S., Downar, J., Vila-Rodriguez, F., Baribeau, D.A., Thorpe, K.E., Daskalakis, Z.J., Blumberger, D.M., 2023. Differential symptom cluster responses to repetitive transcranial magnetic stimulation treatment in depression. *Eclinicalmedicine* 55, 101765.
- Kebets, V., Holmes, A.J., Orban, C., Tang, S., Li, J., Sun, N., Kong, R., Poldrack, R.A., Yeo, B.T.T., 2019. Somatosensory-Motor Dysconnectivity Spans Multiple Transdiagnostic Dimensions of Psychopathology. *Biol. Psychiatry* 86, 779-791.
- Kessler, R.C., Birnbaum, H., Bromet, E., Hwang, I., Sampson, N., Shahly, V., 2010. Age differences in major depression: results from the National Comorbidity Survey Replication (NCS-R). *Psychol. Med.* 40, 225-237.
- Klok, M.P.C., van Eijndhoven, P.F., Argyelan, M., Schene, A.H., Tendolkar, I., 2019. Structural brain characteristics in treatment-resistant depression: review of magnetic resonance imaging studies. *BJPsych Open* 5, e76.
- Kopelman, J., Keller, T.A., Panny, B., Griffo, A., Degutis, M., Spotts, C., Cruz, N., Bell, E., Do-Nguyen, K., Wallace, M.L., 2023. Rapid neuroplasticity changes and response to intravenous ketamine: a randomized controlled trial in

treatment-resistant depression. *Translational Psychiatry* 13, 1-9.

Krishnan, A., Williams, L.J., McIntosh, A.R., Abdi, H., 2011. Partial Least Squares (PLS) methods for neuroimaging: A tutorial and review. *Neuroimage* 56, 455-475.

Lamers, F., Milaneschi, Y., De Jonge, P., Giltay, E., Penninx, B., 2018. Metabolic and inflammatory markers: associations with individual depressive symptoms. *Psychol. Med.* 48, 1102-1110.

Landi, I., Mandelli, V., Lombardo, M.V., 2021. reval: A Python package to determine best clustering solutions with stability-based relative clustering validation. *Patterns* 2, 100228.

Leckman, J.F., Sholomskas, D., Thompson, D., Belanger, A., Weissman, M.M., 1982. Best estimate of lifetime psychiatric diagnosis: a methodological study. *Archives of general psychiatry* 39, 879-883.

Li, J.M., Zhang, Y., Su, W.J., Liu, L.L., Gong, H., Peng, W., Jiang, C.L., 2018a. Cognitive behavioral therapy for treatment-resistant depression: A systematic review and meta-analysis. *Psychiatry Res.* 268, 243-250.

Li, Z.Q., Yan, Z.Y., Lan, F.J., Dong, Y.Q., Xiong, Y., 2018b. Suppression of NLRP3 inflammasome attenuates stress-induced depression-like behavior in NLGN3-deficient mice. *Biochem. Biophys. Res. Commun.* 501, 933-940.

Liang, S., Deng, W., Li, X., Greenshaw, A.J., Wang, Q., Li, M., Ma, X., Bai, T.-J., Bo, Q.-J., Cao, J., 2020. Biotypes of major depressive disorder: neuroimaging evidence from resting-state default mode network patterns. *NeuroImage: Clinical* 28, 102514.

Licinio, J., Frost, P., 2000. The neuroimmune-endocrine axis: pathophysiological implications for the central nervous system cytokines and hypothalamus-pituitary-adrenal hormone dynamics. *Braz. J. Med. Biol. Res.* 33, 1141-1148.

Lippard, E.T., Nemeroff, C.B., 2020. The devastating clinical consequences of child abuse and neglect: increased disease vulnerability and poor treatment response in mood disorders. *Am. J. Psychiatry* 177, 20-36.

Lombardo, M.V., Eyler, L., Pramparo, T., Gazestani, V.H., Hagler, D.J., Chen, C.-H., Dale, A.M., Seidlitz, J., Bethlehem, R.A.I., Bertelsen, N., Barnes, C.C., Lopez, L., Campbell, K., Lewis, N.E., Pierce, K., Courchesne, E., 2021. Atypical genomic cortical patterning in autism with poor early language outcome. *Science Advances* 7, eabh1663.

Lorenzo-Luaces, L., Buss, J.F., Fried, E.I., 2021. Heterogeneity in major depression and its melancholic and atypical specifiers: a secondary analysis of STAR* D. *BMC psychiatry* 21, 1-11.

Mandelli, V., Landi, I., Busuoli, E.M., Courchesne, E., Pierce, K., Lombardo, M.V., 2023. Prognostic early snapshot stratification of autism based on adaptive functioning. *Nature Mental Health* 1, 327-336.

Mannarino, A.P., Cohen, J.A., Deblinger, E., 2014. Trauma-focused cognitive-behavioral therapy. Evidence-based

approaches for the treatment of maltreated children: Considering core components and treatment effectiveness, 165-185.

McAllister-Williams, R.H., Arango, C., Blier, P., Demyttenaere, K., Falkai, P., Gorwood, P., Hopwood, M., Javed, A., Kasper, S., Malhi, G.S., Soares, J.C., Vieta, E., Young, A.H., Papadopoulos, A., Rush, A.J., 2020. The identification, assessment and management of difficult-to-treat depression: An international consensus statement. *J. Affect. Disord.* 267, 264-282.

McInnes, L., Healy, J., Melville, J., 2018. Umap: Uniform manifold approximation and projection for dimension reduction. arXiv preprint arXiv:1802.03426.

Milaneschi, Y., Lamers, F., Berk, M., Penninx, B.W., 2020. Depression heterogeneity and its biological underpinnings: toward immunometabolic depression. *Biol. Psychiatry* 88, 369-380.

Miola, A., Meda, N., 2023. Structural and functional features of treatment-resistant depression: A systematic review and exploratory coordinate-based meta-analysis of neuroimaging studies. *Psychiatric Clinical Neuroscience* 77, 256-263.

Mori, S., Oishi, K., Jiang, H., Jiang, L., Li, X., Akhter, K., Hua, K., Faria, A.V., Mahmood, A., Woods, R., 2008. Stereotaxic white matter atlas based on diffusion tensor imaging in an ICBM template. *Neuroimage* 40, 570-582.

Nanni, V., Uher, R., Danese, A., 2012. Childhood maltreatment predicts unfavorable course of illness and treatment outcome in depression: a meta-analysis. *Am. J. Psychiatry* 169, 141-151.

Nusslock, R., Miller, G.E., 2016. Early-life adversity and physical and emotional health across the lifespan: A neuroimmune network hypothesis. *Biol. Psychiatry* 80, 23-32.

Olgiate, P., Serretti, A., 2022. Post-traumatic stress disorder and childhood emotional abuse are markers of subthreshold bipolarity and worse treatment outcome in major depressive disorder. *International clinical psychopharmacology* 37, 1.

Osimo, E.F., Pillinger, T., Rodriguez, I.M., Khandaker, G.M., Pariante, C.M., Howes, O.D., 2020. Inflammatory markers in depression: A meta-analysis of mean differences and variability in 5,166 patients and 5,083 controls. *Brain. Behav. Immun.* 87, 901-909.

Pandit, V., Swain, A.K., Yadav, P., 2022. Comparison of Dimensionality Reduction and Clustering Methods for Single-Cell Transcriptomics Data. *bioRxiv*, 2022.2010. 2015.512334.

Papadopoulos, A.S., Cleare, A.J., 2012. Hypothalamic–pituitary–adrenal axis dysfunction in chronic fatigue syndrome. *Nature Reviews Endocrinology* 8, 22-32.

Paul, E.R., Östman, L., Heilig, M., Mayberg, H.S., Hamilton, J.P., 2023. Towards a multilevel model of major

- depression: genes, immuno-metabolic function, and cortico-striatal signaling. *Transl. Psychiatry* 13, 171.
- Pelin, H., Ising, M., Stein, F., Meinert, S., Meller, T., Brosch, K., Winter, N.R., Krug, A., Leenings, R., Lemke, H., 2021. Identification of transdiagnostic psychiatric disorder subtypes using unsupervised learning. *Neuropsychopharmacology* 46, 1895-1905.
- Price, J.L., Drevets, W.C., 2012. Neural circuits underlying the pathophysiology of mood disorders. *TICS* 16, 61-71.
- Quitkin, F.M., Stewart, J.W., Mcgrath, P.J., Tricamo, E., Rabkin, J.G., Ocepek-Welikson, K., Nunes, E., Harrison, W., Klein, D.F., 1993. Columbia atypical depression: a subgroup of depressives with better response to MAOI than to tricyclic antidepressants or placebo. *The British Journal of Psychiatry* 163, 30-34.
- Rasmussen, L.J.H., Moffitt, T.E., Arseneault, L., Danese, A., Eugen-Olsen, J., Fisher, H.L., Harrington, H., Houts, R., Matthews, T., Sugden, K., Williams, B., Caspi, A., 2020. Association of Adverse Experiences and Exposure to Violence in Childhood and Adolescence With Inflammatory Burden in Young People. *JAMA Pediatrics* 174, 38-47.
- Rethorst, C.D., Tu, J., Carmody, T.J., Greer, T.L., Trivedi, M.H., 2016. Atypical depressive symptoms as a predictor of treatment response to exercise in Major Depressive Disorder. *J. Affect. Disord.* 200, 156-158.
- Reynolds, W.M., Gould, J.W., 1981. A psychometric investigation of the standard and short form Beck Depression Inventory. *J. Consult. Clin. Psychol.* 49, 306.
- Rost, N., Dwyer, D.B., Gaffron, S., Rechberger, S., Maier, D., Binder, E.B., Brückl, T.M., 2023. Multimodal predictions of treatment outcome in major depression: A comparison of data-driven predictors with importance ratings by clinicians. *J. Affect. Disord.*
- Rothermundt, M., Arolt, V., Peters, M., Gutbrodt, H., Fenker, J., Kersting, A., Kirchner, H., 2001. Inflammatory markers in major depression and melancholia. *J. Affect. Disord.* 63, 93-102.
- Runia, N., Yücel, D.E., Lok, A., de Jong, K., Denys, D., van Wingen, G.A., Bergfeld, I.O., 2022. The neurobiology of treatment-resistant depression: A systematic review of neuroimaging studies. *Neurosci. Biobehav. Rev.* 132, 433-448.
- Rush, A.J., Aaronson, S.T., Demyttenaere, K., 2019. Difficult-to-treat depression: A clinical and research roadmap for when remission is elusive. *Aust. N. Z. J. Psychiatry* 53, 109-118.
- Rush, A.J., Trivedi, M.H., Wisniewski, S.R., Nierenberg, A.A., Stewart, J.W., Warden, D., Niederehe, G., Thase, M.E., Lavori, P.W., Lebowitz, B.D., McGrath, P.J., Rosenbaum, J.F., Sackeim, H.A., Kupfer, D.J., Luther, J., Fava, M., 2006. Acute and longer-term outcomes in depressed outpatients requiring one or several treatment steps: a STAR*D report. *Am. J. Psychiatry* 163, 1905-1917.

- Sackeim, H.A., 2001. The definition and meaning of treatment-resistant depression. *J. Clin. Psychiatry* 62, 10-17.
- Schmitgen, M.M., Kubera, K.M., Depping, M.S., Nolte, H.M., Hirjak, D., Hofer, S., Hasenkamp, J.H., Seidl, U., Stieltjes, B., Maier-Hein, K.H., 2020. Exploring cortical predictors of clinical response to electroconvulsive therapy in major depression. *Eur. Arch. Psychiatry Clin. Neurosci.* 270, 253-261.
- Sforzini, L., Worrell, C., Kose, M., Anderson, I.M., Aouizerate, B., Arolt, V., Bauer, M., Baune, B.T., Blier, P., Cleare, A.J., 2022. A Delphi-method-based consensus guideline for definition of treatment-resistant depression for clinical trials. *Mol. Psychiatry* 27, 1286-1299.
- Shapiro, F., 2001. Eye movement desensitization and reprocessing (EMDR): Basic principles, protocols, and procedures. Guilford Press.
- Silverstein, B., Angst, J., 2015. Evidence for broadening criteria for atypical depression which may define a reactive depressive disorder. *Psychiatry journal* 2015.
- Smith, S.M., 2002. Fast robust automated brain extraction. *Hum. Brain Mapp.* 17, 143-155.
- Smith, S.M., Jenkinson, M., Johansen-Berg, H., Rueckert, D., Nichols, T.E., Mackay, C.E., Watkins, K.E., Ciccarelli, O., Cader, M.Z., Matthews, P.M., 2006. Tract-based spatial statistics: voxelwise analysis of multi-subject diffusion data. *Neuroimage* 31, 1487-1505.
- Soares, H.D., Potter, W.Z., Pickering, E., Kuhn, M., Immermann, F.W., Shera, D.M., Ferm, M., Dean, R.A., Simon, A.J., Swenson, F., Siuciak, J.A., Kaplow, J., Thambisetty, M., Zagouras, P., Koroshetz, W.J., Wan, H.I., Trojanowski, J.Q., Shaw, L.M., Biomarkers Consortium Alzheimer's Disease Plasma Proteomics Project, f.t., 2012. Plasma Biomarkers Associated With the Apolipoprotein E Genotype and Alzheimer Disease. *Arch. Neurol.* 69, 1310-1317.
- Soczynska, J.K., Kennedy, S.H., Alsuwaidan, M., Mansur, R.B., Li, M., McAndrews, M.P., Brietzke, E., Woldeyohannes, H.O., Taylor, V.H., McIntyre, R.S., 2017. A pilot, open-label, 8-week study evaluating the efficacy, safety and tolerability of adjunctive minocycline for the treatment of bipolar I/II depression. *Bipolar Disorders* 19, 198-213.
- Stewart, J.W., 2007. Treating depression with atypical features. *Journal of clinical psychiatry* 68, 25-29.
- Strawbridge, R., Arnone, D., Danese, A., Papadopoulos, A., Herane Vives, A., Cleare, A.J., 2015. Inflammation and clinical response to treatment in depression: A meta-analysis. *Eur. Neuropsychopharmacol.* 25, 1532-1543.
- Strawbridge, R., Hodsoll, J., Powell, T.R., Hotopf, M., Hatch, S.L., Breen, G., Cleare, A.J., 2019. Inflammatory profiles of severe treatment-resistant depression. *J. Affect. Disord.* 246, 42-51.

- Sullivan, P.F., Neale, M.C., Kendler, K.S., 2000. Genetic epidemiology of major depression: review and meta-analysis. *Am. J. Psychiatry* 157, 1552-1562.
- Taraku, B., Woods, R.P., Boucher, M., Espinoza, R., Jog, M., Al-Sharif, N., Narr, K.L., Zavaliangos-Petropulu, A., 2023. Changes in white matter microstructure following serial ketamine infusions in treatment resistant depression. *Hum. Brain Mapp.* 44, 2395-2406.
- Teicher, M.H., Gordon, J.B., Nemeroff, C.B., 2022. Recognizing the importance of childhood maltreatment as a critical factor in psychiatric diagnoses, treatment, research, prevention, and education. *Mol. Psychiatry* 27, 1331-1338.
- Thase, M.E., Rush, A.J., 1997. When at first you don't succeed: sequential strategies for antidepressant nonresponders. *J. Clin. Psychiatry* 58, 23-29.
- Tokuda, T., Yoshimoto, J., Shimizu, Y., Okada, G., Takamura, M., Okamoto, Y., Yamawaki, S., Doya, K., 2018. Identification of depression subtypes and relevant brain regions using a data-driven approach. *Sci. Rep.* 8, 14082.
- Van Velzen, L.S., Kelly, S., Isaev, D., Aleman, A., Aftanas, L.I., Bauer, J., Baune, B.T., Brak, I.V., Carballedo, A., Connolly, C.G., 2020. White matter disturbances in major depressive disorder: a coordinated analysis across 20 international cohorts in the ENIGMA MDD working group. *Mol. Psychiatry* 25, 1511-1525.
- Vignali, D.A., 2000. Multiplexed particle-based flow cytometric assays. *J. Immunol. Methods* 243, 243-255.
- Vreijling, S.R., van Haeringen, M., Milaneschi, Y., Huider, F., Bot, M., Amin, N., Beulens, J.W., Bremmer, M.A., Elders, P.J., Galesloot, T.E., 2023. Sociodemographic, lifestyle and clinical characteristics of energy-related depression symptoms: A pooled analysis of 13,965 depressed cases in 8 Dutch cohorts. *J. Affect. Disord.* 323, 1-9.
- Wen, J., Fu, C.H., Tosun, D., Veturi, Y., Yang, Z., Abdulkadir, A., Mamourian, E., Srinivasan, D., Skampardon, I., Singh, A., 2022. Characterizing heterogeneity in neuroimaging, cognition, clinical symptoms, and genetics among patients with late-life depression. *JAMA psychiatry* 79, 464-474.
- Wild, E., Magnusson, A., Lahiri, N., Krus, U., Orth, M., Tabrizi, S.J., Björkqvist, M., 2011. Abnormal peripheral chemokine profile in Huntington's disease. *PLoS currents* 3, Rm1231.
- Wiles, N., Thomas, L., Abel, A., Ridgway, N., Turner, N., Campbell, J., Garland, A., Hollinghurst, S., Jerrom, B., Kessler, D., 2013. Cognitive behavioural therapy as an adjunct to pharmacotherapy for primary care based patients with treatment resistant depression: results of the CoBaIT randomised controlled trial. *The Lancet* 381, 375-384.
- Williams, L.M., Debattista, C., Duchemin, A.M., Schatzberg, A.F., Nemeroff, C.B., 2016. Childhood trauma predicts antidepressant response in adults with major depression: data from the randomized international study to predict

optimized treatment for depression. *Transl. Psychiatry* 6, e799.

Withers, A.C., Tarasoff, J.M., Stewart, J.W., 2013. Is depression with atypical features associated with trauma history? *The Journal of clinical psychiatry* 74, 500-506.

Wong, M.L., Insera, A., Lewis, M.D., Mastronardi, C.A., Leong, L., Choo, J., Kentish, S., Xie, P., Morrison, M., Wesselingh, S.L., Rogers, G.B., Licinio, J., 2016. Inflammasome signaling affects anxiety- and depressive-like behavior and gut microbiome composition. *Mol. Psychiatry* 21, 797-805.

Yang, Y., Sun, H., Zhang, Y., Zhang, T., Gong, J., Wei, Y., Duan, Y.-G., Shu, M., Yang, Y., Wu, D., 2021. Dimensionality reduction by UMAP reinforces sample heterogeneity analysis in bulk transcriptomic data. *Cell reports* 36, 109442.

Yeung, H.W., Shen, X., Stolicyn, A., De Nooij, L., Harris, M.A., Romaniuk, L., Buchanan, C.R., Waiter, G.D., Sandu, A.L., McNeil, C.J., 2021. Spectral clustering based on structural magnetic resonance imaging and its relationship with major depressive disorder and cognitive ability. *Eur. J. Neurosci.* 54, 6281-6303.

Zanardi, R., Carminati, M., Attanasio, F., Fazio, V., Maccario, M., Colombo, C., 2024. How different definition criteria may predict clinical outcome in treatment resistant depression: Results from a prospective real-world study. *Psychiatry Res.* 334, 115818.

Zhou, L., Wang, L., Wang, M., Dai, G., Xiao, Y., Feng, Z., Wang, S., Chen, G., 2022. Alterations in white matter microarchitecture in adolescents and young adults with major depressive disorder: A voxel-based meta-analysis of diffusion tensor imaging. *Psychiatry research. Neuroimaging* 323, 111482.

Zhou, Y., Zhao, L., Zhou, N., Zhao, Y., Marino, S., Wang, T., Sun, H., Toga, A.W., Dinov, I.D., 2019. Predictive big data analytics using the UK biobank data. *Sci. Rep.* 9, 1-10.

Zimmerman, M., Ellison, W., Young, D., Chelminski, I., Dalrymple, K., 2015. How many different ways do patients meet the diagnostic criteria for major depressive disorder? *Compr. Psychiatry* 56, 29-34.

Accepted Author Manuscript
European Neuropsychopharmacology, 2024 Aug;
<https://doi.org/10.1016/j.euroneuro.2024.05.015>